

## Linear elastic and limit state solutions of beam string structures by the Ritz-method

Weichen Xue\* and Sheng Liu

*Department of Building Engineering, Tongji University, Shanghai 200092, China*

*(Received September 27, 2007, Accepted January 19, 2010)*

**Abstract.** The beam string structure (BSS) has been widely applied in large span roof structures, while no analytical solutions of BSS were derived for it in the existing literature. In the first part of this paper, calculation formulas of displacement and internal forces were obtained by the Ritz-method for the most commonly used arc-shaped BSS under the vertical uniformly distributed load and the prestressing force. Then, the failure mode of BSS was proposed based on the static equilibrium. On condition the structural stability was reliable, BSS under the uniformly distributed load would fail by tensile strength failure of the string, and the beam remained in the elastic or semi-plastic range. On this basis, the limit load of BSS was given in virtue of the elastic solutions. In order to verify the linear elastic and limit state solutions proposed in this paper, three BSS modal were tested and the corresponding elastoplastic large deformation analysis was performed by the ANSYS program. The proposed failure mode of BSS was proved to be correct, and the analytical results for the linear elastic and limit state were in good agreement with the experimental and FEM results.

**Keywords:** beam string structure; Ritz method; limit state; failure mode; ANSYS; modal test; elastoplastic large deformation analysis.

---

### 1. Introduction

In 1984, Prof. Masao Saitoh first proposed the concept of beam string structure (BSS), which is a self-balancing system formed by combining compression-bending beam and tension string (Fig. 1) (Saitoh and Tosiya 1985). Stiffened and prestressed by the high tensile strength string, the members of BSS can be arranged to achieve the best use of their individual material properties. As a result, BSS is a light-weight structure which bears the capacity of covering a large span (Levy *et al.* 1994). Up to the present, BSS has been widely applied in large span roofs of stadiums, public halls and aeroplane hangers, mainly in Japan and China. Maehashi Green Dome, Izumo Dome, Anoh Dome (Saitoh and Okasa 1999), Shanghai Pudong International Airport, Guangzhou International Exhibition Center and Harbin International Sports, Exhibition Center (Huang 2005) and Shanghai Yuanshen Arena (Liu 2007) are some typical BSS roof structures.

In the late 1980s, based on a set of model tests, Masao Saitoh found that BSS developed larger load carrying capacity than the common rigid beam or truss structures (Saitoh and Ohtake 1988,

---

\*Corresponding author, Professor, E-mail: [xuewc@tongji.edu.cn](mailto:xuewc@tongji.edu.cn)

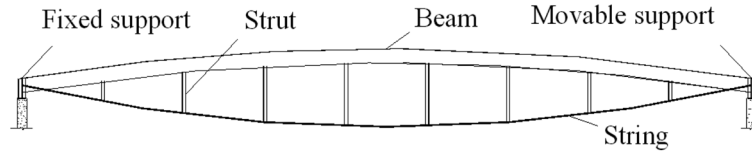


Fig. 1 Schematic of BSS

Saitoh 1988). In 1994, Some Japanese scholars discussed the role of the string in hybrid string structure (HSS, including BSS) (Saitoh and Okasa 1999, Hosozawa *et al.* 1999). In the same year, Masao Saitoh studied the mechanical characteristics of a light-weight complex structure composed of a membrane and a beam string structure (Saitoh *et al.* 1994). With the construction of some large-span BSS roofs in the last two decades, a series of research work of BSS roofs has been conducted in China. In 1999, the full-scale static test (Chen *et al.* 1999) and 1:20 scale model shaking-table test (Li *et al.* 1999) were carried out for the BSS roof of Shanghai Pudong International Airport. Nevertheless, these works mentioned above are all concerned with the experimental or numerical studies of BSS, yet no analytical solutions have been derived. On the other hand, the previous works mostly deal with the elastic behavior of BSS, while the topic of elastic-plastic behavior has been little covered, and the research of failure mode still remains blank yet.

The so-called Ritz method (1908) is a frequently used variational method in structural analysis. This method has been applied in solving boundary value and eigenvalue problems especially for some simple members such as beams, plates and so on. The objective of this paper is to obtain the linear elastic and limit state solutions via the Ritz method for BSS, which is a complicated structure composed of the compression-bending beam, tension string and compression struts.

## 2. Research significance

This paper mainly focuses on the most commonly used arc-shaped BSS. In the first part, the linear elastic solutions for BSS under the vertical uniformly distributed load and prestressing force are derived by the Ritz method. Second, the failure mode of BSS under the uniformly distributed vertical load is analyzed, and the corresponding calculation formulas for the limit load are given in virtue of the elastic solutions. The solutions proposed in this paper can be applied in the design and analysis of BSS.

## 3. Linear elastic solutions

### 3.1 Problem definition and the Ritz method

Consider an arc-shaped BSS (as shown in Fig. 2) of span  $L$ , rise  $f_1$ , rag  $f_2$ . The modules of elasticity, area and moment of inertial of the beam are  $E_1$ ,  $A_1$  and  $I_1$ , respectively. The modules of elasticity and area of the string are  $E_2$  and  $A_2$ , respectively.

Generally, in order to control the deformations and internal forces of BSS under the dead load, the prestressing force is introduced in the string intentionally before extra vertical load applied. The

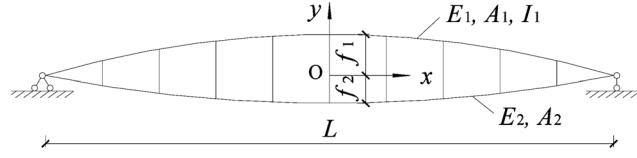


Fig. 2 Schematic of an arc-shaped BSS

prestressing force  $T_0$  (prestressing force in a broad sense) which occurs in a string can be indicated as the sum of the tensile force  $T_e$  (existing tensile force) caused by the equilibrium and the tensile force  $T_p$  (prestressing force in a narrow sense) which is introduced intentionally to control the behavior (Saitoh and Okasa 1999).

$$T_0 = T_e + T_p \quad (1)$$

The value of  $T_e$  changes depending on the self weight of BSS during the stretching phase, structural system and degree of redundancy. Since the structural rigidity and boundary conditions are quite different under the vertical load (including the load applied during the stretching as well as the additional load applied after the stretching) and the prestressing force, these two effects should be analyzed separately and then superimposed together.

The Ritz method is based on the following ideas. The displacement functions of BSS are given as a certain kind of series

$$w(x) = \sum_{i=1}^n w_i y_i(x), \quad u(x) = \sum_{i=1}^n u_i f_i(x) \quad (2)$$

where  $y_i(x)$  and  $f_i(x)$  are linearly independent functions which satisfy the geometric boundary conditions, and  $w_i$  and  $u_i$  are as yet unknown real constants.  $w(x)$  and  $u(x)$  are also called the base functions.

The total potential energy (strain energy plus load energy) of BSS can be given by  $\Pi(w_1, w_2, \dots, w_n, u_1, u_2, \dots, u_n, f)$  where  $f$  is the external load.

According to the principle of the minimum of the potential energy, the functional  $\Pi$  is minimized by simply taking the partial derivatives

$$\frac{\partial \Pi}{\partial w_i} = 0, \quad \frac{\partial \Pi}{\partial u_i} = 0 \quad (i = 1, 2, \dots, n) \quad (3)$$

And the system is uniquely solvable (Rektorys 1979).

The following assumptions are adopted in the analysis:

- The materials are linear elastic.
- The struts keep up-right.
- The shear deformation of the beam is not considered.
- The string is not capable of carrying bending loads.

Note that the positive values denote the upward and rightward displacement, the tensile force and the upward external force.

### 3.2 Strain energy

Consider a micro-segment AB in Fig. 3. The initial length is  $ds_0 = \sqrt{(dx)^2 + (dy)^2}$ . After

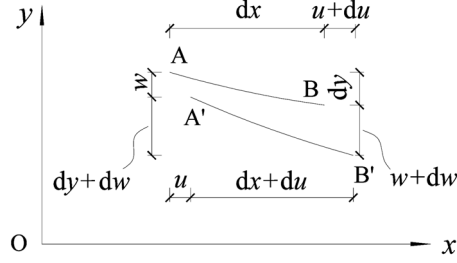


Fig. 3 Schematic of the deformation of a micro-segment

deformation, the length changes to  $ds = \sqrt{(dx + du)^2 + (dy + dw)^2}$ , the axial strain is given by

$$\begin{aligned}\varepsilon &= \frac{ds - ds_0}{ds_0} = \frac{\sqrt{(dx + du)^2 + (dy + dw)^2} - \sqrt{(dx)^2 + (dy)^2}}{\sqrt{(dx)^2 + (dy)^2}} \\ &= \frac{1}{\sqrt{1 + \left(\frac{dy}{dx}\right)^2}} \left[ \sqrt{1 + 2\frac{du}{dx} + \left(\frac{du}{dx}\right)^2 + \left(\frac{dy}{dx}\right)^2 + 2\frac{dy}{dx} \cdot \frac{dw}{dx} + \left(\frac{dw}{dx}\right)^2} - \sqrt{1 + \left(\frac{dy}{dx}\right)^2} \right] \\ &\approx \frac{1}{\sqrt{1 + \left(\frac{dy}{dx}\right)^2}} \left[ \frac{du}{dx} + \frac{dy}{dx} \cdot \frac{dw}{dx} + \frac{1}{2} \left(\frac{dw}{dx}\right)^2 \right]\end{aligned}\quad (4)$$

The axial force of the micro-segment is

$$N = EA\varepsilon \quad (5)$$

And  $N$  and  $ds$  can be also given by

$$N = H \sec \theta \quad (6)$$

$$ds = \sec \theta dx \quad (7)$$

where  $H$  is the horizontal component of the axial force  $N$ , and  $\sec \theta = \sqrt{1 + \left(\frac{dy}{dx}\right)^2}$   
Hence the axial strain energy is

$$U_N = \frac{1}{2} \int N \varepsilon dx = \frac{1}{2} \int H \varepsilon \sec^2 \theta dx \quad (8)$$

The bending strain energy is

$$U_M = \frac{1}{2} \int EI \left( \frac{d^2 w}{dx^2} \right)^2 dx \quad (9)$$

### 3.3 Solutions under the vertical uniformly distributed load

Consider a BSS under a uniformly distributed load  $q$ , as shown in Fig. 4. The initial shapes of the beam and string are both arcs: the beam is

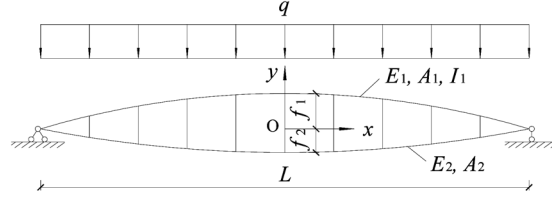


Fig. 4 Schematic of a BSS under a uniformly distributed load

$$x^2 + \left(y - \frac{f_1}{2} + \frac{L^2}{8f_1}\right)^2 = \left(\frac{f_1}{2} + \frac{L^2}{8f_1}\right)^2 = R_1^2 \quad (10)$$

and the string is

$$x^2 + \left(y + \frac{f_2}{2} - \frac{L^2}{8f_2}\right)^2 = \left(\frac{f_2}{2} + \frac{L^2}{8f_2}\right)^2 = R_2^2 \quad (11)$$

where  $R_1$  and  $R_2$  are the curvature radius of the beam and string, respectively.

By symmetry, the horizontal displacement of the mid-span of the BSS is assumed to be zero. Consequently, the base functions of the BSS can be given as the following Fourier series

$$w = \sum w_n \cos \frac{n\pi x}{L}, \quad u = \sum u_n \sin \frac{n\pi x}{L}, \quad n = 1, 3, 5, \dots \quad (12)$$

The single dimensional bases are adopted here, which were quite similar to the deformation of BSS

$$w = w_1 \cos \frac{\pi x}{L}, \quad u = u_1 \sin \frac{\pi x}{L} \quad (13)$$

As mentioned already, the struts are assumed to be upright, so the horizontal components of axial forces of each segment of the string are equal. Accordingly

$$\begin{aligned} H &= \frac{1}{L} \int_{-L/2}^{L/2} H dx \\ &= \int_{-L/2}^{L/2} \frac{E_2 A_2 \varepsilon_2}{L} \frac{1}{\sqrt{1 + \left(\frac{dy}{dx}\right)^2}} dx \\ &= \frac{E_2 A_2}{L} \int_{-L/2}^{L/2} \frac{1}{\sqrt{1 + \left(\frac{dy}{dx}\right)^2}} \left[ \frac{du}{dx} + \frac{dy}{dx} \cdot \frac{dw}{dx} + \frac{1}{2} \left(\frac{dw}{dx}\right)^2 \right] \frac{1}{\sqrt{1 + \left(\frac{dy}{dx}\right)^2}} dx \\ &= \frac{2\pi E_2 A_2}{R_2^2 L^2} \left\{ \int_0^{L/2} u_1 \left(y + \frac{f_2}{2} - \frac{L^2}{8f_2}\right)^2 \cos \frac{\pi x}{L} dx + \int_0^{L/2} \frac{\pi w_1^2 \left(y + \frac{f_2}{2} - \frac{L^2}{8f_2}\right)^2 \sin^2 \frac{\pi x}{L}}{2L} dx \right. \\ &\quad \left. - R_2 w_1 \int_0^{L/2} \sqrt{1 - \left(\frac{x}{R_2}\right)^2} x \sin \frac{\pi x}{L} dx \right\} \quad (14) \end{aligned}$$

Further, some simplifications are made for Eq. (14)

$$\cos \frac{\pi x}{L} \approx 1 - \frac{\pi^2 x^2}{2L^2} + \frac{\pi^4 x^4}{24L^4}, \quad \sin^2 \frac{\pi x}{L} \approx \left( \frac{\pi x}{L} - \frac{\pi^3 x^3}{6L^3} \right)^2, \quad \sqrt{1 - \left( \frac{x}{R_2} \right)^2} \approx 1 - \frac{x^2}{2R_2^2} - \frac{x^4}{8R_2^4}$$

and  $x = R_2 \cos \theta$ ,  $y + \frac{f_2}{2} - \frac{L^2}{8f_2} = R_2 \sin \theta$

where,  $\theta \in \left( \frac{3\pi}{2}, \frac{3\pi}{2} + \theta_0 \right)$ ,  $\theta_0 = \arcsin \frac{L}{2R_2}$

After the simplification, we have

$$H = K_1 u_1 + K_2 w_1 + K_3 w_1^2 \quad (15)$$

where  $K_1$ ,  $K_2$  and  $K_3$  are some constants as follows

$$\begin{aligned} K_1 &= \frac{2\pi R_2 E_2 A_2}{L^2} \left[ \sin \theta_0 - \left( \frac{\pi^2 R_2^2}{2L^2} + 1 \right) \frac{\sin^3 \theta_0}{3} + \left( \frac{\pi^4 R_2^4}{24L^4} + \frac{\pi^2 R_2^2}{2L^2} \right) \frac{\sin^5 \theta_0}{5} - \frac{\pi^4 R_2^4 \sin^7 \theta_0}{168L^4} \right] \\ K_2 &= \frac{2\pi E_2 A_2}{R_2 L} \left[ -\frac{L}{\pi^2} + \frac{1}{2R_2^2} \left( \frac{3}{4\pi^2} - \frac{6}{\pi^4} \right) L^3 + \frac{1}{8R_2^4} \left( \frac{5}{16\pi^2} - \frac{15}{\pi^4} + \frac{120}{\pi^6} \right) L^5 \right] \\ K_3 &= \frac{\pi^2 R_2 E_2 A_2}{L^3} \left[ \frac{(\pi^2 R_2^2 + L^2) \sin^3 \theta_0}{3L^2} + \left( \frac{\pi^4 R_2^4}{3L^4} + \frac{\pi^2 R_2^2}{L^2} \right) \frac{\sin^5 \theta_0}{5} + \left( \frac{\pi^6 R_2^6}{36L^6} + \frac{\pi^4 R_2^4}{3L^4} \right) \frac{\sin^7 \theta_0}{7} - \frac{\pi^6 R_2^6 \sin^9 \theta_0}{36L^6 \cdot 9} \right] \end{aligned}$$

Hence, the strain energy of the strain is

$$\begin{aligned} U_2 &= \frac{1}{2} H \int_{-L/2}^{L/2} \varepsilon_2 \sec^2 \theta dx \\ &= \frac{1}{2} H \int_{-L/2}^{L/2} \frac{1}{\sqrt{1 + \left( \frac{dy}{dx} \right)^2}} \left[ \frac{du}{dx} + \frac{dy}{dx} \cdot \frac{dw}{dx} + \frac{1}{2} \left( \frac{dw}{dx} \right)^2 \right] \left[ 1 + \left( \frac{dy}{dx} \right)^2 \right] dx \\ &= \frac{\pi H}{L} \int_0^{L/2} \left\{ u_1 \cos \frac{\pi x}{L} \left[ 1 - \left( \frac{x}{R_2} \right)^2 \right]^{-1/2} - \frac{w_1}{R_2} x \left[ 1 - \left( \frac{x}{R_2} \right)^2 \right] \sin \frac{\pi x}{L} + \frac{\pi w_1^2 \left[ 1 - \left( \frac{x}{R_2} \right)^2 \right]^{-1/2} \sin^2 \frac{\pi x}{L}}{2L} \right\} dx \quad (16) \end{aligned}$$

Simplified by using the Taylor's series, we obtain

$$U_2 = \frac{1}{2} (K_1 u_1 + K_2 w_1 + K_3 w_1^2) (K'_1 u_1 + K'_2 w_1 + K'_3 w_1^2) \quad (17)$$

where  $K'_1 = 2 + \frac{1}{2R_2^2} \left( \frac{1}{2} - \frac{4}{\pi^2} \right) L^2 - \frac{3}{8R_2^4} \left( \frac{1}{8} - \frac{6}{\pi^2} + \frac{48}{\pi^4} \right) L^4$ ,  $K'_2 = \left( \frac{3}{2\pi} - \frac{12}{\pi^3} \right) \frac{L^3}{R_2^3} - \frac{2L}{\pi R_2}$

$$K'_3 = \frac{\pi^2}{4L} + \frac{\pi^2}{2R_2^2} \left( \frac{1}{48} + \frac{1}{8\pi^2} \right) L - \frac{3\pi^2}{8R_2^4} \left( \frac{1}{320} + \frac{1}{16\pi^2} - \frac{3}{8\pi^4} \right) L^3$$

Analogously, the axial strain energy of the beam is given by

$$U_{1N} = \frac{1}{2}(J_1 u_1 + J_2 w_1 + J_3 w_1^2)(J'_1 u_1 + J'_2 w_1 + J'_3 w_1^2) \quad (18)$$

$$\text{where } J_1 = \frac{2\pi R_1 E_1 A_1}{L^2} \left[ \sin \theta_{B0} - \left( \frac{\pi^2 R_1^2}{2L^2} + 1 \right) \frac{\sin^3 \theta_{B0}}{3} + \left( \frac{\pi^4 R_1^4}{24L^4} + \frac{\pi^2 R_1^2}{2L^2} \right) \frac{\sin^5 \theta_{B0}}{5} - \frac{\pi^4 R_1^4 \sin^7 \theta_{B0}}{168L^4} \right]$$

$$J_2 = \frac{2\pi E_1 A_1}{R_1 L} \left[ \frac{L}{\pi^2} - \frac{1}{2R_1^2} \left( \frac{3}{4\pi^2} - \frac{6}{\pi^4} \right) L^3 - \frac{1}{8R_1^4} \left( \frac{5}{16\pi^2} - \frac{15}{\pi^4} + \frac{120}{\pi^6} \right) L^5 \right]$$

$$J_3 = \frac{\pi^2 R_1 E_1 A_1}{L^3} \left[ \frac{(\pi^2 R_1^2 + L^2) \sin^3 \theta_{B0}}{3L^2} + \left( \frac{\pi^4 R_1^4}{3L^4} + \frac{\pi^2 R_1^2}{L^2} \right) \frac{\sin^5 \theta_{B0}}{5} + \left( \frac{\pi^6 R_1^6}{36L^6} + \frac{\pi^4 R_1^4}{3L^4} \right) \frac{\sin^7 \theta_{B0}}{7} - \frac{\pi^6 R_1^6 \sin^9 \theta_{B0}}{36L^6 \cdot 9} \right]$$

$$\sin \theta_{B0} = \frac{2L}{R_1}, J'_1 = 2 + \frac{1}{2R_1^2} \left( \frac{1}{2} - \frac{4}{\pi^2} \right) L^2 - \frac{3}{8R_1^4} \left( \frac{1}{8} - \frac{6}{\pi^2} + \frac{48}{\pi^4} \right) L^4, J'_2 = \frac{2L}{\pi R_1} - \left( \frac{3}{2\pi} - \frac{12}{\pi^3} \right) \frac{L^3}{R_1^3}$$

$$J'_3 = \frac{\pi^2}{4L} + \frac{\pi^2}{2R_1^2} \left( \frac{1}{48} + \frac{1}{8\pi^2} \right) L - \frac{3\pi^2}{8R_1^4} \left( \frac{1}{320} + \frac{1}{16\pi^2} - \frac{3}{8\pi^4} \right) L^3$$

The bending strain energy of the beam is

$$U_{1M} = \frac{1}{2} \int_{-L/2}^{L/2} E_1 I_1 \left( \frac{d^2 w}{dx^2} \right)^2 dx = \frac{1}{2} \int_{-L/2}^{L/2} \frac{\pi^4 E_1 I_1 w_1^2}{L^4} \cos^2 \frac{\pi x}{L} dx = \frac{\pi^4 E_1 I_1 w_1^2}{4L^3} \quad (19)$$

The load energy is

$$W_q = \int_{-L/2}^{L/2} q w dx = q w_1 \int_{-L/2}^{L/2} \cos \frac{\pi x}{L} dx = \frac{2q w_1 L}{\pi} \quad (20)$$

So the total potential energy of the BSS can be given by

$$\begin{aligned} \Pi &= U_{1N} + U_{1M} + U_2 - W_q \\ &= \frac{1}{2}(J_1 u_1 + J_2 w_1 + J_3 w_1^2)(J'_1 u_1 + J'_2 w_1 + J'_3 w_1^2) + \frac{\pi^4 E_1 I_1 w_1^2}{4L^3} \\ &\quad + \frac{1}{2}(K_1 u_1 + K_2 w_1 + K_3 w_1^2)(K'_1 u_1 + K'_2 w_1 + K'_3 w_1^2) - \frac{2q w_1 L}{\pi} \end{aligned} \quad (21)$$

According to the principle of the minimum of the potential energy, we have  $\partial \Pi / \partial w_1 = 0$ ,  $\partial \Pi / \partial u_1 = 0$ , i.e., the system

$$\left. \begin{aligned} h_1 u_1 + h_2 w_1 + h_3 u_1 w_1 + h_4 w_1^2 + h_5 w_1^3 &= h_6 \\ h_7 u_1 + h_8 w_1 + h_9 w_1^2 &= 0 \end{aligned} \right\} \quad (22)$$

$$\text{where } h_1 = h_8 = \frac{1}{2} J_1 J'_2 + \frac{1}{2} J_2 J'_1 + \frac{1}{2} K_1 K'_2 + \frac{1}{2} K_2 K'_1, h_2 = J_2 J'_2 + \frac{\pi^4 E_1 I_1}{2L^3} + K_2 K'_2$$

$$h_3 = 2h_9 = J_1J'_3 + J_3J'_1 + K_1K'_3 + K_3K'_1, \quad h_4 = \frac{3}{2}(J_2J'_3 + J_3J'_2 + K_2K'_3 + K_3K'_2)$$

$$h_5 = 2(J_3J'_3 + K_3K'_3), \quad h_6 = \frac{2qL}{\pi}, \quad h_7 = J_1J'_1 + K_1K'_1$$

Further, we have

$$\left(h_5 - \frac{h_3h_9}{h_7}\right)w_1^3 + \left(-\frac{h_1h_9}{h_7} - \frac{h_3h_8}{h_7} + h_4\right)w_1^2 + \left(-\frac{h_1h_8}{h_7} + h_2\right)w_1 - h_6 = 0 \quad (23)$$

As a matter of fact, when the displacement is relatively small, the load and displacement are almost in a linear relationship. Thus, we neglect the higher-order items  $w_1^3$  and  $w_1^2$ , and obtain

$$\left. \begin{aligned} w_1 &= Eq \\ u_1 &= -\frac{h_8}{h_7}w_1 = -\frac{h_8}{h_7}Eq \end{aligned} \right\} \quad (24)$$

where  $E$  is the equivalent rigidity of the BSS,  $E = \frac{2L}{\pi\left(h_2 - \frac{h_1h_8}{h_7}\right)}$ .

Applying Eq. (25) in Eq. (15) and Eq. (6), and neglecting the higher-order items, we obtain the axial force of the beam and string

$$\left. \begin{aligned} N_1 &= \frac{1}{2}(J_1u_1 + J_2w_1)\sec\theta = \frac{1}{2}(J_1u_1 + J_2w_1)\frac{R_1}{\sqrt{R_1^2 - x^2}} \\ N_2 &= \frac{1}{2}(K_1u_1 + K_2w_1)\sec\theta = \frac{1}{2}(K_1u_1 + K_2w_1)\frac{R_2}{\sqrt{R_2^2 - x^2}} \end{aligned} \right\} \quad (25)$$

and the bending moment of the beam

$$M = EI\frac{d^2w}{dx^2} = -\frac{\pi^2 EIw_1}{L^2}\cos\frac{\pi x}{L} \quad (26)$$

### 3.4 Solutions under the prestressing force

As shown in Fig. 5, the beam is separated as our subject of study, while the effective prestressing force  $H$  in the string and the supporting forces of the struts are considered as external forces applied to the beam. The supporting forces of the struts are simplified as a uniformly distributed load  $q = 2H\sin\theta_{B0}/L$ , where  $\theta_{B0}$  is the included angle of  $H$  and the horizontal direction.

By symmetry, the horizontal displacement of the mid-span of the BSS is assumed to be zero. Consequently, the base functions of the BSS can be given as the following one dimensional Fourier series

$$w = w_{10}\cos\frac{\pi x}{L}, \quad u = u_{10}\sin\frac{\pi x}{L} \quad (27)$$



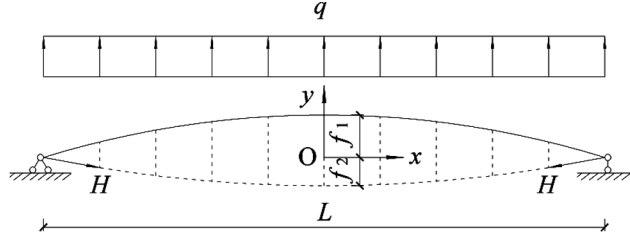


Fig. 5 Schematic of a BSS under the prestressing force

The strain energy of the beam is given by

$$U_1 = U_{1N} + U_{1M} = \frac{1}{2}(J_1 u_{10} + J_2 w_{10} + J_3 w_{10}^2)(J'_1 u_{10} + J'_2 w_{10} + J'_3 w_{10}^2) + \frac{\pi^4 E_1 I_1 w_{10}^2}{4L^3} \quad (28)$$

Hence the total potential energy of the beam is

$$\begin{aligned} \Pi &= U_1 - W \\ &= \frac{1}{2}(J_1 u_{10} + J_2 w_{10} + J_3 w_{10}^2)(J'_1 u_{10} + J'_2 w_{10} + J'_3 w_{10}^2) + \frac{\pi^4 E_1 I_1 w_{10}^2}{4L^3} - 2H u_{10} \cos \theta_{B0} - \frac{2q w_{10} L}{\pi} \end{aligned} \quad (29)$$

Applying the principle of the minimum of the potential energy, we have  $\partial \Pi / \partial w_{10} = 0$ ,  $\partial \Pi / \partial u_{10} = 0$ , i.e., the system

$$\left. \begin{aligned} h_{10} u_{10} + h_{20} w_{10} + h_{30} u_{10} w_{10} + h_{40} w_{10}^2 + h_{50} w_{10}^3 &= h_{60} \\ h_{70} u_{10} + h_{80} w_{10} + h_{90} w_{10}^2 &= h_{100} \end{aligned} \right\} \quad (30)$$

where  $h_{10} = h_{80} = \frac{1}{2} J_1 J'_2 + \frac{1}{2} J_2 J'_1$ ,  $h_{20} = J_2 J'_2 + \frac{\pi^4 E_1 I_1}{2L^3}$ ,  $h_{30} = 2h_{90} = J_1 J'_3 + J_3 J'_1$

$$h_{40} = \frac{3}{2}(J_2 J'_3 + J_3 J'_2), \quad h_{50} = 2J_3 J'_3, \quad h_{60} = \frac{2qL}{\pi} = \frac{4H \sin \theta_{B0}}{\pi}, \quad h_{70} = J_1 J'_1, \quad h_{100} = 2H \cos \theta_{B0}$$

The experimental results showed that when the displacement is relatively small, the prestressing force and displacement are almost in a linear relationship. Thus, we neglect the higher-order items, and obtain

$$\left. \begin{aligned} w_{10} &= E_0 H \\ u_{10} &= \left( \frac{\cos \theta_{B0}}{h_{70}} - \frac{h_{80}}{h_{70}} E_0 \right) H \end{aligned} \right\} \quad (31)$$

where,  $E_0$  is the equivalent rigidity of the beam under the prestressing force

$$E_0 = \left( \frac{4 \sin \theta_{B0}}{\pi} - \frac{h_{10} \cos \theta_{B0}}{h_{70}} \right) / \left( -\frac{h_{10} h_{80}}{h_{70}} + h_{20} + \frac{h_{100} h_{30}}{h_{70}} \right)$$

Since the beam is statically determinated, hence its internal forces can be obtained by static equilibrium directly.

## 4. Limit state solutions

### 4.1 Failure mode

From the viewpoint of static equilibrium, BSS is a self-balancing system, i.e., the horizontal components of the axial forces of the beam and string are equal. Generally, for the sake of architectural effects, the rise to span ratio of the beam and the rag to span ratio of the string are conventionally very close to each other. Consequently, the axial forces of the beam and string are quite close.

On the other hand, in real BSS roof structures, the area of the beam cross section is usually 8 to 20 times the area of the string cross section (Huang 2005, Liu 2007), while the limit strength of the soft steel used in the beam is commonly about a quarter of the limit strength of the high tensile cables used in the string. So when the string reaches its strength limit, the end segments of the beam near the supports, where the moments are relatively low, still remain in the elastic range. And the middle segments of the beam, whose moments are relatively high, are under the following two possible states:

- Entirely remain elastic
- Partially or entirely enter the plastic range

If the beam remains elastic, the BSS will fail by the tensile strength failure of the string. And then, we only need to consider the latter state. The typical stress-strain curves of the soft steel used in the beam and the hard steel of the string are presented in Fig. 6. It can be seen that the limit strain of the soft steel (10% or higher) is much higher than the hard steel (4% to 7%). As a matter of fact, the commonly used cable in BSS consists of a number of parallel or twisted high-strength wires. Caused by the possible initial imperfection and uneven distribution of stress, the limit strength and limit strain of a cable is much lower than those of a single wire. The test results (Fu *et al.* 2000) of the cables taken from the Williamsburg Bridge (by Steinman in 1988 and Biebiek in 1990, respectively) showed that the limit strain of those cables was only about 0.03. As mentioned already, when the string reaches its strength limit, the end segments of the beam remain elastic. Restricted by the elastic zone, the strain of the plastic zone of the beam is unable to develop freely. So, the maximum strain of the beam remains in the same order of magnitude as the elastic zone, and the stress of the beam is much lower than the limit stress.

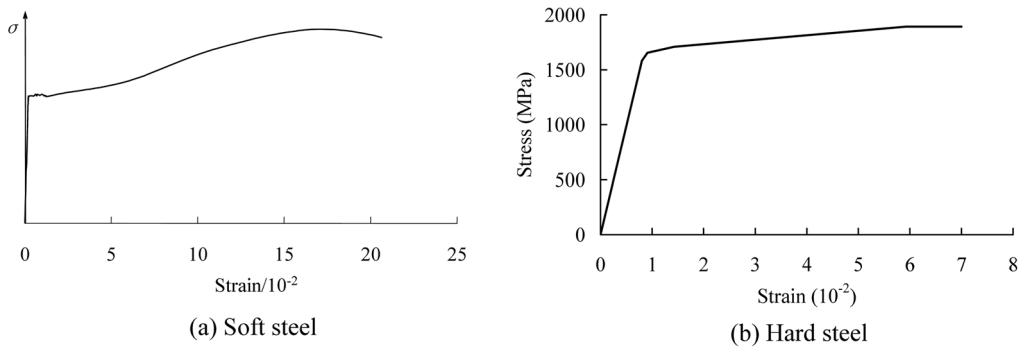


Fig. 6 The stress-strain curves of soft steel and hard steel

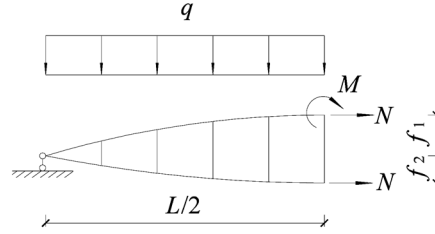


Fig. 7 Semi-structure analytical model

Consequently, we can come to the conclusion that, on condition that the structural stability is reliable after lateral braces applied, the failure mode of BSS is the tensile strength failure of the string, and the beam remains in the elastic or semi-plastic range.

#### 4.2 Ultimate load

Consider a semi-structure under a uniformly distributed load  $q$ , as shown in Fig. 7.

By equilibrium of bending moments at the support, we have

$$\frac{1}{8}qL^2 = N \cdot (f_1 + f_2) + M \quad (32)$$

so

$$N = \frac{1}{f_1 + f_2} \left( \frac{qL^2}{8} - M \right) \quad (33)$$

Note that, the sectional rigidity of the beam is a small part of the global rigidity of the BSS. Accordingly, the bending moment of the beam  $M$  is much smaller than the bending moment of the BSS  $qL^2/8$ . Thus, although  $M$  and the vertical load  $q$  are in a nonlinear relationship,  $N$  can be approximately considered linear to  $q$ , we obtain

$$N = kq \quad (34)$$

Further, the ultimate load of the BSS

$$q_u = F_u A_2 / k \quad (35)$$

where  $k$  can be given by the linear elastic solutions proposed already

$$k = \frac{L \left( K_2 - \frac{J_1 J'_2 + J_2 J'_1 + K_1 K'_2 + K_2 K'_1}{2(J_1 J'_1 + K_1 K'_1)} K_1 \right)}{\pi \left( J_2 J'_2 + \frac{\pi^4 E_1 I_1}{2L^3} + K_2 K'_2 - \frac{(J_1 J'_2 + J_2 J'_1 + K_1 K'_2 + K_2 K'_1)^2}{4(J_1 J'_1 + K_1 K'_1)} \right)} \quad (36)$$

and  $F_u$  is the ultimate stress of the string.

## 5. Experimental and FEM verification

In order to verify the linear elastic and limit state solutions proposed in this paper, three scaled BSS specimens (BSS-1~BSS-2 (Xue and Liu 2009) and BSS-3 (Li 2007)) were tested, and corresponding elastoplastic large deformation analysis was conducted. In addition, the stretching test of the full-scale BSS specimen (BSS-4 (Chen *et al.* 1999)) of Shanghai Pudong International Airport was also served as verification. The design parameters and material properties of specimens are presented in Table 1 and Table 2, respectively.

The primary process of the stretching was the following:

- Installation of the equipments for stretching.
- Application of the extra mass load.
- Stretching.
- Anchoring.

The loading installations of the tests are shown in Fig. 8 and Fig. 9. In order to assure the stability of the specimens, several lateral braces were applied. Load sensors were set under each hydraulic jack to obtain the accurate load values.

Table 1 Design parameters of specimens

Specimens	$L$ (mm)	$f_1$ (mm)	$f_2$ (mm)	Beam (mm)	String (mm)	Struts (mm)	$E_1$ (MPa)	$E_2$ (MPa)
BSS-1	7000	280	385	□ 60×40×2	2φ5	φ18	$2.06 \times 10^5$	$2.08 \times 10^5$
BSS-2	7000	350	385	□ 60×40×2	2φ5	φ18	$2.06 \times 10^5$	$2.08 \times 10^5$
BSS-3	7000	700	350	φ76×2	1φ5	φ18	$1.85 \times 10^5$	$2.08 \times 10^5$
BSS-4	84140	5160	6540	□ 600×400×18 +2 □ 300×300×6	241φ5	350×10	$2.06 \times 10^5$	$1.85 \times 10^5$

Table 2 Measured material properties for specimens

Specimen	Members	$F_y$ (MPa)	$F_u$ (MPa)	$E_1$ (MPa)	$E_2$ (MPa)	Elongation (%)
BSS-1	Beam	322	371	$2.06 \times 10^5$	$2.08 \times 10^5$	10.0
	String	1582	1873			7.0
BSS-2	Beam	370	450	$2.06 \times 10^5$	$2.08 \times 10^5$	14.3
	String	1582	1873			7.0
BSS-3	Beam	224	461	$1.85 \times 10^5$	$2.08 \times 10^5$	9.5
	String	1582	1873			7.0
BSS-4	Beam	325	550	$2.05 \times 10^5$	$1.85 \times 10^5$	21.0
	String	1330	1570			4.0

Note that the beams of BSS-1~BSS-3 composed of cold-rolled forming steel sections, so the elongations of the beams of BSS-1~BSS-3 are relatively lower than the commonly used soft steel

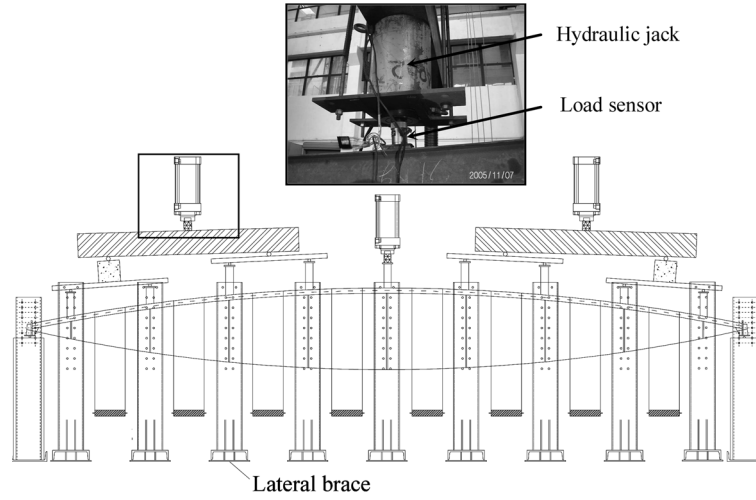


Fig. 8 Loading installation of tests

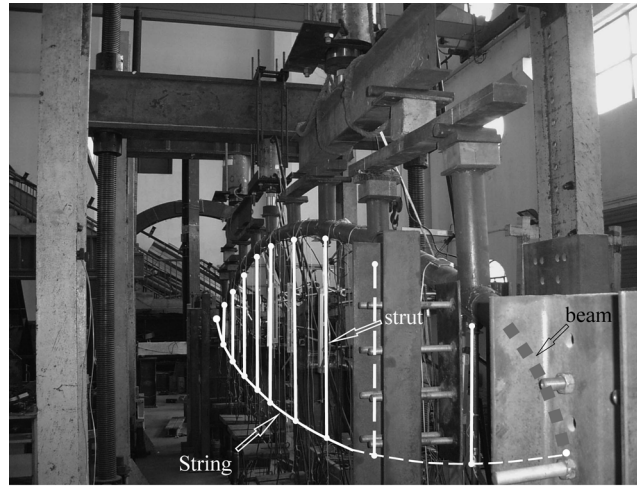


Fig. 9 Loading test of the specimens

### 5.1 Verification of linear elastic solutions

Table 3 presents the comparison of the analytical results, experimental results and the FEM results in elastic stage, and a good agreement can be observed.

### 5.2 Verifications of limit state solutions

#### 5.2.1 Failure mode

In order to verify the failure mode and the corresponding calculation formulas proposed in this paper, specimens BSS-1~BSS-3 were loaded to the limit state. Fig. 10 to Fig. 15 show the experimental and FEM strain curves of the beam and string of the three specimens. We can see that,

when the specimens fail, the stresses of the string grow quite close to the ultimate stress (the strains of the string are larger than  $9000 \mu\epsilon$ , for BSS-1, the strains are even higher than  $13000 \mu\epsilon$ , which means the stresses are up to 1600 MPa or higher from Fig. 6(b)), the stresses of the beam are still in the elastic range or slightly higher than the yielding stress (the strains are lower than  $2000 \mu\epsilon$ ). That is in good agreement with the failure mode proposed already.

Table 3 Comparison of analytical results, experimental results and FEM results

Specimen	Results	Stretching phase		Vertical load bearing phase				
		$T_0$ (kN)	camber (mm)	Load (kN/m)	$v$ (mm)	$N_1$ (kN)	$M_1$ (kN·m)	$N_2$ (kN)
BSS-1	Ana.	7.34	21.18	2.35	-12.45	-21.62	0.09	21.66
	Exp.	7.34	20.75	2.35	-13.91	-19.44	0.11	21.76
	FEM	7.34	20.50	2.35	-13.98	-18.84	0.12	22.27
	Ana./ Exp.	-	1.02	-	0.90	1.11	0.82	1.00
	Ana./ FEM	-	1.03	-	0.89	1.15	0.75	0.97
BSS-2	Ana.	6.76	7.45	2.35	-18.06	-20.23	0.13	19.87
	Exp.	6.76	7.21	2.35	-18.89	-17.75	0.15	19.24
	FEM	6.76	7.31	2.35	-16.90	-17.82	0.15	19.74
	Ana./ Exp.	-	1.03	-	0.96	1.14	0.87	1.03
	Ana./ FEM	-	1.02	-	1.07	1.14	0.87	1.01
BSS-3	Ana.	2.76	17.95	1.40	-7.82	-9.35	0.07	9.49
	Exp.	2.76	18.34	1.40	-8.38	-9.90	0.08	9.95
	FEM	2.76	17.70	1.40	-8.27	-9.73	0.08	9.75
	Ana./ Exp.	-	0.98	-	0.93	0.94	0.88	0.95
	Ana./ FEM	-	1.01	-	0.95	0.96	0.88	0.97
BSS-4	Ana.	620	313	-	-	-	-	-
	Exp.	620	320	-	-	-	-	-
	FEM	620	304	-	-	-	-	-
	Ana./ Exp.	-	0.98	-	-	-	-	-
	Ana./ FEM	-	1.03	-	-	-	-	-

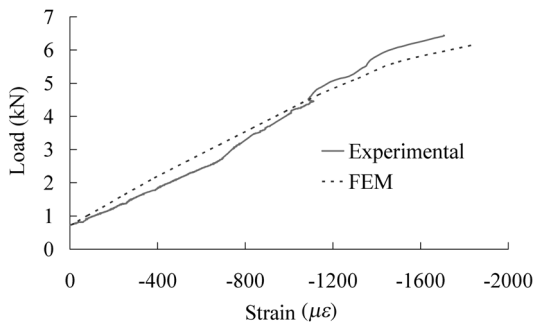


Fig. 10 Maximum beam strain of BSS-1

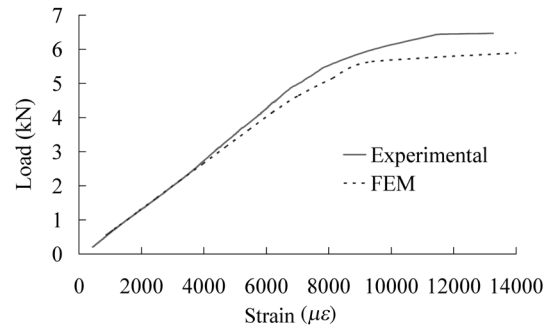


Fig. 11 Maximum string strain of BSS-1

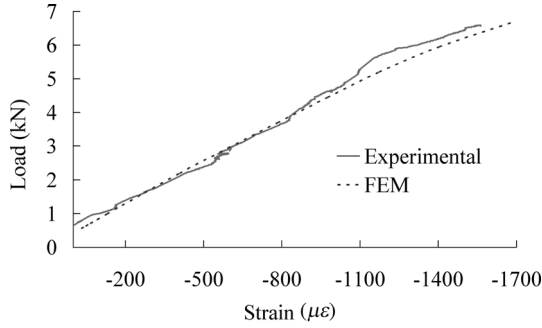


Fig. 12 Maximum beam strain of BSS-2

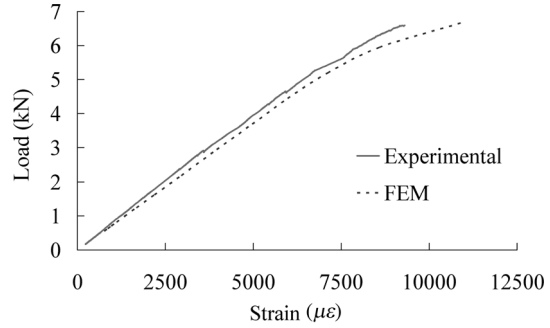


Fig. 13 Maximum string strain of BSS-2

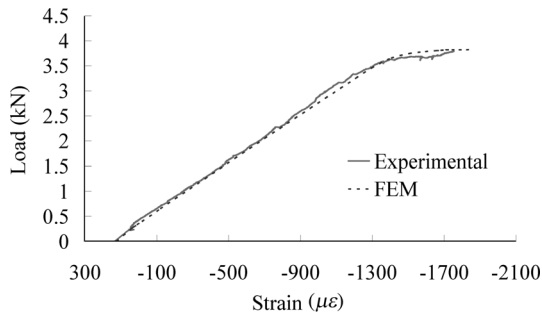


Fig. 14 Maximum beam strain of BSS-3

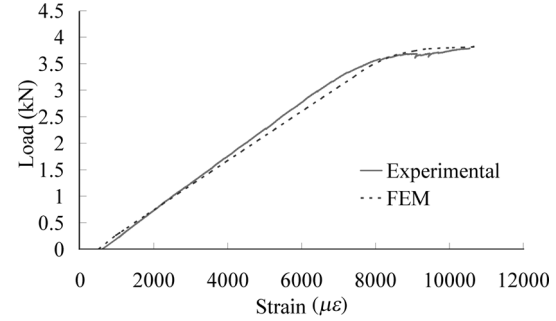


Fig. 15 Maximum string strain of BSS-3

Table 4 Comparison for limit load of analytical, experimental and FEM results

Specimens	Ana. (kN)	Exp. (kN)	FEM (kN)	Ana./Exp.	Ana./FEM
BSS-1	6.15	6.44	6.14	0.95	1.00
BSS-2	6.79	6.59	6.69	1.03	1.01
BSS-3	4.19	3.89	4.23	1.08	0.99

### 5.2.2 Limit load

Table 4 presents the comparison of the analytical, experimental and the FEM results of the limit load of the three specimens, and a good agreement can be observed.

## 6. Conclusions

The linear elastic solutions of conventional arc-shaped BSS were derived by the Ritz method. Based on the failure mode analysis, BSS would fail by the tensile strength failure of the string, and the beam remained in the elastic or semi-plastic range under uniformly distributed load, and on condition the structural stability was reliable. Further, the calculation formulas of the limit load of BSS were obtained in virtue of the elastic solutions.

In order to verify the proposed linear elastic and limit state solutions, this paper conducted the

experimental work on three BSS specimens, and performed the corresponding elastoplastic large deformation analysis. In addition, the stretching test of the full-scale BSS specimen of Shanghai Pudong International Airport was also served as verification. Comparisons showed the analytical, experimental and FEM results were in good agreement.

## Acknowledgements

The work described in this paper was supported by the Open Project in 2005 of Key Lab of RC & PC Structure of Ministry of Education, China.

## References

- Chen, Y., Shen, Z., Zhao, X., Chen, Y., Wang, D., Gao, C. and Chen, H. (1999), "Experimental study on a full-scale roof truss of Shanghai Pudong International Airport Terminal", *J. Buil. Struct.*, **20**(2), 9-17. (In Chinese)
- Fu, G., Moses, F. and Khazem, D.A. (2000), "Strength of parallel wire cables for suspension bridges", *Proceedings of the 8th ASCE Specialty Conference on Probabilistic Mechanics and Structural Reliability*, Notre Dame, July.
- Hosozawa, O., Shimamura, K. and Mizutani, T. (1999), "The role of cables in large span spatial structures: introduction of recent space structures with cables in Japan", *Eng. Struct.*, **21**(8), 795-804.
- Huang, M. (2005), "Design and construction of large-span beam string structures", *ShanDong Science and Technology Press*, Shandong, China. (In Chinese)
- Levy, R., Hanaor, A. and Rizzuto, N. (1994), "Experimental investigation of prestressing in double-layer grids", *Int. J. Space Struct.*, **9**(1), 21-6.
- Li, G., Shen, Z., Ding, X., Zhou, X., Chen, Y., Zhang, F. and Zhou, J. (1999), "Shaking table experimental study on R2 steel roof model of Shanghai Pudong International Airport Terminal subjected to three dimensional earthquakes", *J. Buil. Struct.*, **20**(2), 18-27. (In Chinese)
- Liu, S. (2007), *Studies on Design Theory and Construction Control of Prestressed Beam String Structures*. Master's thesis, Dept. of Building Engineering. Tongji Univ. Shanghai. China.
- Rektorys, K. (1979), "Variational methods in mathematics, science and engineering", D. Reidel Publishing Company, Prague, Czechoslovakia.
- Ritz, W. (1908), "U ber eine neue Methode zur L6sung gewisser Variationsprobleme der mathematischen Physik", *Journal für Reine und Angewandte Mathematik*, **135**, 1-61.
- Saitoh, M. (1988), "A study on structural planning of radial type beam string structures", *Proceedings of the Summaries of Technical Papers of Annual Meeting Architectural Institute of Japan*, Tokyo. (In Japanese)
- Saitoh, M. and Ohtake, T. (1988), "A Study on beam string structure with flat circular arch", *Proceedings of the Summaries of Technical Papers of Annual Meeting Architectural Institute of Japan*, Tokyo. (In Japanese)
- Saitoh, M. and Okasa, A. (1999), "The role of string in hybrid string structure", *Eng. Struct.*, **21**(8), 756-769.
- Saitoh, M. and Tosiya, K. (1985), "A study on structural behaviors of beam string structure", *Proceedings of the Summaries of Technical Papers of Annual Meeting Architectural Institute of Japan*, Tokyo. (In Japanese)
- Saitoh, M., Okada, A., Maejima, K. and Gohda, T. (1994), "Study on mechanical characteristics of a light-weight complex structure composed of a membrane and a beam string structure", *Proceedings of the IASS-ASCE International Symposium 1994 on Spatial, Lattice and Tension Structures*, Atlanta, April.
- Xue, W. and Liu, S. (2009), "Design optimization and experimental study on beam string structures", *J. Constr. Steel Res.*, **65**(1), 70-80.